Synthesis and anticancer activities of 6-amino amonafide derivatives

John T. Norton[a], Mark A. Witschi[c,d], Lynn Luong[b], Akane Kawamura[e], Supurna Ghosh[a], M. Sharon Stack[a], Edith Sim[e], Michael J. Avram[b], Daniel H. Appella[c] and Sui Huang[a]

Amonafide is a DNA intercalator and topoisomerase II inhibitor in clinical development for the treatment of neoplastic diseases. Amonafide contains a free arylamine, which causes it to be metabolized in humans by *N*-acetyl transferase-2 (NAT2) into a toxic form. To eliminate the NAT2 acetylation of amonafide while retaining the anticancer properties, we have synthesized nine derivatives that are structurally similar to amonafide that should not be acetylated. Eight derivatives have arylamines at the 6-position (vs. 5-position of amonafide) and one derivative completely lacks the arylamine. The derivative with a free amine in the 6-position and one with a substituted amine in the 6-position are not acetylated, whereas amonafide is extensively acetylated as determined by an NAT2 assay. The biological activities of these compounds were evaluated to determine whether they behaved similarly to amonafide in purified systems and *in vitro*. We found that three compounds had similar cancer cell-selective growth inhibition to amonafide, while retaining similar subcellular localization, DNA intercalation and topoisomerase II inhibition activities. In addition, these compounds were able to eliminate a marker of metastatic potential, the perinucleolar compartment. These three compounds (named numonafides) might thus allow for better patient management than those treated with amonafide; hence, they should be developed further as potential clinical replacements for amonafide or as novel anticancer drugs. *Anti-Cancer Drugs* 19:23–36

Anti-Cancer Drugs 2008, **19**:23–36

Keywords: amonafide, *N*-acetyl-transferase 2, numonafide, perinucleolar compartment

Departments of [a]Cell and Molecular Biology and [b]Anesthesiology, The Mary Beth Donnelley Clinical Pharmacology Core Facility, Northwestern University Medical School, Chicago, [c]Department of Chemistry, Northwestern University, Evanston, Illinois, [d]National Institutes of Health, NIDDK, Bethesda, Maryland, USA and [e]Department of Pharmacology, University of Oxford, Oxford, UK

Correspondence to Sui Huang, Department of Cell and Molecular Biology, Northwestern University Medical School, 303 E. Chicago Avenue W11-240, Chicago, IL 60611, USA
E-mail: s-huang2@northwestern.edu

Received 9 March 2007 **Revised form accepted** 16 July 2007

Introduction

Amonafide is a DNA intercalator and topoisomerase II (topo II) inhibitor [1–3] that has shown good activity in several clinical trials [4–6]. The malate salt of amonafide is currently under clinical development for the treatment of acute myelocytic leukemia [7] and the dihyrdochloride salt is under clinical development for the treatment of refractory prostate carcinoma [8]. Amonafide is converted into two main metabolites in humans, which are an inactive/nontoxic *N′*-hydroxylated metabolite and an active/toxic *N*-acetyl metabolite [9–13] (Fig. 1a). The latter is produced by *N*-acetyl transferase 2 (NAT2) [12], which is a polymorphic enzyme causing differential acetylation activity among individuals [13]. *N*-acetyl amonafide has been suggested to compete for metabolic inactivation via CYP1A2 (Fig. 1a), with the parent drug causing increased plasma levels of active drug, thereby causing toxicities [9]. Patients who are phenotyped as fast acetylators produce higher levels of the toxic *N*-acetylated metabolite causing increased drug-related toxicities compared with slow acetylators [14]. The extent of this differential acetylation causes some slow acetylators to be severely underdosed and some fast acetylators to experience grade 4 toxicities at a fixed dose [9]. This problem has forced physicians to determine the patient's acetylator status on the basis of caffeine (a substrate for NAT2) acetylation rate [9,15] or by genotyping [8] to optimize the dose of amonafide for each group. These phenotyping/genotyping assays delay treatment and add to the cost of the treatment regimen. In addition, once phenotyped or genotyped, fast acetylators receive a lower dose of amonafide [15], which might decrease the efficacy of amonafide treatment for this group of patients.

A derivative of amonafide that cannot be acetylated, but retains biological activity might allow for consistent treatment regimens in patients independent of acetylator phenotype. This hypothesis has been addressed in previous studies with the creation of the amonafide derivatives, azonafide [16] and mitonafide [17]. Azonafide contains an anthracene ring instead of the naphthalene ring of amonafide and has no free arylamine. Mitonafide has a nitro group in the 5-positon, instead of

0959-4973

Fig. 1

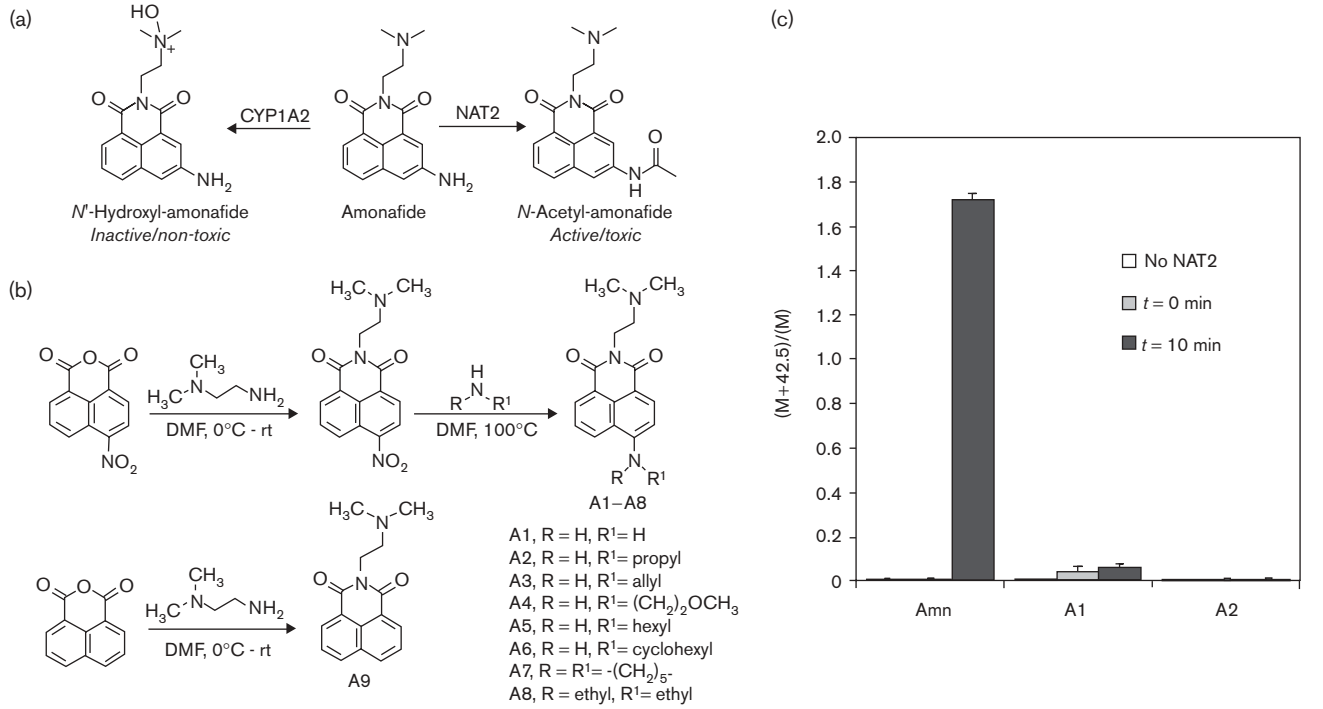

Synthesis of amonafide derivatives and *N*-acetyl transferase-2 (NAT2) assay. (a) CYP1A2 is responsible for the inactivation of amonafide and NAT2 is responsible for the production of the toxic *N*-acetyl species. (b) Synthesis scheme for A1–A9. (c) Recombinant human NAT2 enzyme assay and mass spectrometry were used to demonstrate 6-position amino derivatives cannot be acetylated. Error bars = + SD (n = 3).

the free amine of amonafide. Both these compounds avoid the NAT2-based metabolism owing to the lack of an arylamine and both are effectively cytotoxic to cultured cancer cells [17,18]. Moreover, very potent bis-napthalamide derivatives, including elinafide, that lack an arylamine have been synthesized [19,20]; however, each of the derivatives mentioned is chemically very different from amonafide, which most likely affects the target, cellular uptake, and/or the bioavailability of the drugs. Therefore, there is still a need for an amonafide derivative that is not able to be metabolized by NAT2, but is chemically similar to amonafide and retains the potency, selectivity and biological activity of amonafide.

The main objective of our studies is to synthesize a derivative of amonafide that cannot be acetylated by NAT2, while maintaining biological activities similar to, or better than, amonafide. We synthesized such derivatives by moving the free arylamine from the 5-position to the 6-position, by adding functional groups to the 6-position amine or by completely removing the arylamine. Nine derivatives were synthesized and the biological activities of each were directly compared with amonafide and other pertinent controls using purified systems and in-vitro assays.

Methods

Chemical synthesis

A total of eight amonafide derivatives with amines in the 6-position were synthesized (A1–A8) in addition to a derivative completely lacking an arylamine (A9). The synthesis scheme is shown in Fig. 1b and the synthesis details are listed below. A1 and A9 have been synthesized previously [17,21]. Amonafide was obtained from the National Cancer Institute's Developmental Therapeutics Program (Bethesda, Maryland, USA). All compounds were stored at 10 mmol/l in dimethyl sulfoxide (DMSO) at −20°C.

Analysis of synthetic products

Proton nuclear magnetic resonances (^{1}H NMRs) were recorded in deuterated solvents on a Gemini 300 (300 MHz; Varian, Palo Alto, California, USA) or an iNOVA 500 (500 MHz; Varian) spectrometer. Chemical shifts are reported in parts per million (p.p.m., δ) relative to tetramethylsilane (δ 0.00). If tetramethylsilane was not present, the residual protio solvent was referenced ($CDCl_3$, δ 7.27; DMSO-d_6, δ 2.50). ^{1}H NMR splitting patterns are designated as singlet (s), doublet (d), triplet (t) or quartet (q). Splitting patterns that could not be interpreted or easily visualized were designated as

multiplet (m) or broad (br). In some cases, the signals from exchangeable protons could not be identified. Coupling constants are reported in Hertz (Hz). Mass spectra were obtained using an API 3000 LC/MS/MS system (Applied Biosystems, Foster City, California, USA), a Micromass Quattro II Triple Quadrupole HPLC/MS/MS mass spectrometer (Waters, Milford, Massachusetts, USA) or a Waters LCT Premier time-of-flight mass spectrometer (Waters). Analytical thin-layer chromatography was carried out on Sorbent Technologies thin-layer chromatography plates precoated with silica gel (250-μm layer thickness; Atlanta, Georgia, USA). Flash column chromatography was performed on EM Science silica gel 60 [230–400 mesh; silica gel 60 (EMD, La Jolla, California, USA)]. All commercially available reagents and solvents were purchased from Aldrich (St Louis, Missouri, USA), and used without further purification except for dimethylformamide (DMF), which was purified by passage through a bed of activated alumina.

Synthesis of 6-nitro-imide precursor (6–nitro-2-[2-(dimethylamino)ethyl]-1H-benz[de] isoquinoline-1,3(2H)-dione)

6-Nitro-naphthylic anhydride (1 g, 4.11 mmol) was dissolved in DMF (40 ml) and the solution was cooled to 0°C, and *N*,*N*-dimethylethylene diamine (0.45 ml, 4.11 mmol) was added drop by drop. The solution was allowed to warm to room temperature and stirred for 24 h. The solvent was removed under vacuum and purified by flash column chromatography to yield 1.24 g (96%) 4-nitro-*N*-(dimethylaminoethyl)naphthylic imide as a light brown solid. ^{1}H NMR (500 MHz, $CDCl_3$) 8.84 (d, $J = 8.0$ Hz, 1H, naphthylic-H) 8.40 (d, $J = 7.5$ Hz, 1H, naphthylic-H) 8.69 (d, $J = 8.0$ Hz, 1H, naphthylic-H) 8.40 (d, $J = 8.0$ Hz, 1H, naphthylic-H) 7.99 (t, $J = 8.0$ Hz, 1H, naphthylic-H) 4.34 (t, $J = 7.0$ Hz, 2H, ethylene-CH_2) 2.67 (t, $J = 7.0$ Hz, 2H, ethylene-CH_2) 2.34 [s, 6H, N(CH_3)$_2$]. Calculated mass for $[M + H]^+ = 314.11$; observed = 314.2.

Synthesis of A1 (6-amino-2-[2-(dimethylamino)ethyl]-1H-benz[de]isoquinoline-1,3(2H)-dione)

Nitro-*N*-(dimethylaminoethyl)naphthalic imide (200 mg, 0.64 mmol) was dissolved in 95% ethanol and slowly added to a Parr flask containing 10% Pd/C. The mixture was placed on a Parr apparatus under 40 psi H_2 pressure for 12 h. The mixture was filtered through Celite and the solvent was removed under vacuum. 6-Nitro-*N*-(dimethylaminoethyl)naphthalic imide was reduced via hydrogenolysis to yield 185 mg (99%) A1 as a bright orange solid. ^{1}H NMR (300 MHz, $CDCl_3$) δ 8.57 (d, $J = 7.0$ Hz, 1H, naphthylic-H) 8.34 (d, $J = 8.0$ Hz, 1H, naphthylic-H) 8.05 (d, $J = 8.5$ Hz, 1H, naphthylic-H) 7.62 (t, 1H, naphthylic-H) 6.79 (d, $J = 8.0$ Hz, 1H, naphthylic-H) 5.04 (br s, 2H, amino-H) 4.32 (t, $J = 6.5$ Hz, 2H, ethylene-CH_2) 2.68 (t, $J = 6.5$ Hz, 2H, ethylene-CH_2) 2.38 [s, 6H, N(CH_3)$_2$]. Calculated mass for $(M + H)^+ = 284.14$; observed = 284.14.

Synthesis of A2 (6-propylamino-2-[2-(dimethylamino) ethyl]-1H-benz[de]isoquinoline-1,3(2H)-dione)

6-Nitro-imide precursor (1 g, 3.19 mmol) was added to a high-pressure vessel and the solid was suspended in DMF (2 ml). Excess propylamine (1 ml) was added, turning the suspension dark brown. The vessel was tightly sealed and heated to 100°C for 1 h. The solution was cooled to room temperature and the solvents were removed under vacuum. The dark brown residue was purified by flash column chromatography (5% MeOH/CH_2Cl_2) to yield 548 mg (53%) of A2 as a bright orange solid. This procedure was used for A3–A8 as well. ^{1}H NMR (500 MHz, $CDCl_3$) δ 8.58 (d, $J = 7.0$ Hz, 1H, naphthylic-H) 8.47 (d, $J = 8.5$ Hz, 1H, naphthylic-H) 8.08 (d, $J = 8.5$ Hz, 1H, naphthylic-H) 7.62 (t, $J = 8.0$ Hz, 1H, naphthylic-H) 6.73 (d, $J = 8.5$ Hz, 1H, naphthylic-H) 5.24 (br s, 1H, amino-H) 4.33 (t, $J = 7.0$ Hz, 2H, ethylene-CH_2) 3.39 (m, 2H, NHCH_2CH_2CH_3) 2.69 (t, $J = 7.0$ Hz, 2H, ethylene-CH_2) 2.40 (s, 6H, N(CH_3)$_2$) 1.85 (m, 2H, NHCH_2CH_2CH_3) 1.12 (t, $J = 7.0$ Hz, 3H, NHCH_2 CH_2CH_3). Calculated mass for $[M + H]^+ = 326.19$; observed = 326.1.

Synthesis of A3 (6-allylamino-2-[2-(dimethylamino) ethyl]-1H-benz[de]isoquinoline-1,3(2H)-dione)

6-Nitro-imide precursor (200 mg, 0.64 mmol) and excess allylamine (0.5 ml) in DMF (1 ml), were reacted to yield 89.4 mg (43%) of A3 as a bright orange solid. ^{1}H NMR (300 MHz, $CDCl_3$) δ 8.59 (dd, $J = 7.2$ Hz, 1H, naphthylic-H) 8.46 (d, $J = 8.4$ Hz, 1H, naphthylic-H) 8.10 (dd, $J = 7.8$ Hz, 1H, naphthylic-H) 7.63 (dd, $J = 7.8$ Hz, 1H, naphthylic-H) 6.73 (d, $J = 8.4$ Hz, 1H, naphthylic-H) 6.10-6.00 (ddt, 1H, CH_2CHCH_2) 5.45-5.30 (m, 2H, terminal alkene-H) 4.32 (t, $J = 7.2$ Hz, 2H, ethylene-CH_2) 3.39 (m, 2H, allylic-H) 2.65 (t, $J = 7.2$ Hz, 2H, ethylene-CH_2) 2.40 [s, 6H, N(CH_3)$_2$]. Calculated mass for $[M + H]^+ = 324.40$; observed = 324.5.

Synthesis of A4 (6-methoxyethylamino-2-[2-(dimethylamino)ethyl]-1H-benz[de]isoquinoline-1,3(2H)-dione)

6-Nitro-imide precursor (200 mg, 0.64 mmol) and excess 2-methoxyethylamine (0.5 ml) in DMF (1 ml) were reacted to yield 33.8 mg (15.5%) of A4 as a bright orange solid. ^{1}H NMR (300 MHz, $CDCl_3$) δ 8.59 (d, $J = 7.5$ Hz, 1H, naphthylic-H) 8.46 (d, $J = 8.7$ Hz, 1H, naphthylic-H) 8.13 (d, $J = 7.5$ Hz, 1H, naphthylic-H) 7.63 (t, $J = 7.8$ Hz, 1H, naphthylic-H) 6.72 (d, $J = 8.7$ Hz, 1H, naphthylic-H) 5.66 (br m, 1H, amino-H) 4.32 (t, $J = 7.2$ Hz, 2H, ethylene-CH_2) 3.78 (m, $J = 5.4$ Hz, 2H, NHCH_2CH_2OCH_3) 3.58 (m, $J = 5.4$ Hz, 2H, NHCH_2CH_2OCH_3) 3.47 (s, 3H, NHCH_2CH_2OCH_3) 2.65 (t, $J = 7.2$ Hz, 2H, ethylene-CH_2) 2.37 (s, 6H,

$N(C\underline{H}_3)_2$). Calculated mass for $[M + H]^+ = 342.18$; observed = 342.18.

Synthesis of A5 (6-hexylamino-2-[2-(dimethylamino) ethyl]-1H-benz[de]isoquinoline-1,3(2H)-dione)

6-Nitro-imide precursor (200 mg, 0.64 mmol) and excess hexylamine (0.5 ml) in DMF (1 ml) were reacted to yield 81.0 mg (34%) of A5 as a bright orange solid. ^{1}H NMR (300 MHz, $CDCl_3$) δ 8.57 (d, $J = 7.5$ Hz, 1H, naphthylic-H) 8.45 (d, $J = 8.4$ Hz, 1H, naphthylic-H) 8.07 (d, $J = 8.7$ Hz, 1H, naphthylic-H) 7.61 (t, $J = 7.5$ Hz, 1H, naphthylic-H) 6.71 (d, $J = 8.4$ Hz, 1H, naphthylic-H) 5.25 (br t, 1H, amino-H) 4.32 (t, $J = 7.2$ Hz, 2H, ethylene-$C\underline{H}_2$) 3.40 (q, $J = 7.2$ Hz, 2H, $NHC\underline{H}_2(CH_2)_4CH_3$) 2.66 (t, $J = 6.9$ Hz, 2H, ethylene-$C\underline{H}_2$) 2.38 (s, 6H, $N(C\underline{H}_3)_2$) 1.81 (m, 2H, hexyl-H) 1.55-1.35 (m, 6H, hexyl-H) 0.93 [t, $J = 6.9$ Hz, 3H, $NHCH_2(CH_2)_4C\underline{H}_3$]. Calculated mass for $[M + H]^+ = 368.50$; observed = 368.0.

Synthesis of A6 (6-cyclohexylamino-2-[2-(dimethylamino) ethyl]-1H-benz[de]isoquinoline-1,3(2H)-dione)

6-Nitro-imide precursor (200 mg, 0.64 mmol) and excess cyclohexylamine (0.5 ml) in DMF (1 ml) were reacted to yield 104 mg (45%) of A6 as a bright orange solid. ^{1}H NMR (300 MHz, $CDCl_3$) δ 8.58 (d, $J = 7.2$ Hz, 1H, naphthylic-H) 8.44 (d, $J = 8.4$ Hz, 1H, naphthylic-H) 8.05 (d, $J = 8.4$ Hz, 1H, naphthylic-H) 7.60 (t, $J = 8.4$ Hz, 1H, naphthylic-H) 6.74 (d, $J = 8.7$ Hz, 1H, naphthylic-H) 5.16 (br d, 1H, amino-H) 4.31 (t, $J = 7.5$ Hz, 2H, ethylene-$C\underline{H}_2$) 3.62 (m, 1H, NHC<u>H</u>-cyclohexyl) 2.65 (t, $J = 6.3$ Hz, 2H, ethylene-$C\underline{H}_2$) 2.37 [s, 6H, $N(C\underline{H}_3)_2$] 2.19 (m, 2H, cyclohexyl-$C\underline{H}_2$) 1.90-1.30 (m, 8H, cyclohexyl-$C\underline{H}_2$). Calculated mass for $[M + H]^+ = 366.49$; observed = 366.0.

Synthesis of A7 (6-piperdinyl-2-[2-(dimethylamino) ethyl]-1H-benz[de]isoquinoline-1,3(2H)-dione)

6-Nitro-imide precursor (200 mg, 0.64 mmol) and excess piperidine (0.5 ml) in DMF (1 ml) were reacted to yield 204 mg (91%) of A7 as a bright orange solid. ^{1}H NMR (300 MHz, $CDCl_3$) δ 8.57 (dd, $J = 7.2$ Hz, 1H, naphthylic-H) 8.49 (d, $J = 8.1$ Hz, 1H, naphthylic-H) 8.39 (dd, $J = 8.4$ Hz, 1H, naphthylic-H) 7.67 (dd, $J = 8.4$ Hz, 1H, naphthylic-H) 7.17 (d, $J = 8.1$ Hz, 1H, naphthylic-H) 4.32 (t, $J = 7.2$ Hz, 2H, ethylene-$C\underline{H}_2$) 3.23 (m, 2H, piperdinyl-H) 2.65 (t, $J = 7.2$ Hz, 2H, ethylene-$C\underline{H}_2$) 2.36 (s, 6H, $N(C\underline{H}_3)_2$) 1.90-1.60 (m, 6H, piperdinyl-H). Calculated mass for $[M + H]^+ = 352.20$; observed = 352.20.

Synthesis of A8 (6-diethylamino-2-[2-(dimethylamino) ethyl]-1H-benz[de]isoquinoline-1,3(2H)-dione)

6-Nitro-imide precursor (200 mg, 0.64 mmol) was treated with excess diethylamine (0.5 ml) in DMF (1 ml) to yield 55.6 mg (26%) of A8 as a bright orange solid. ^{1}H NMR (300 MHz, $CDCl_3$) δ 8.58 (dd, $J = 7.2$ Hz, 1H, naphthylic-H) 8.49 (d, $J = 8.4$ Hz, 1H, naphthylic-H) 8.45 (dd, $J = 8.4$ Hz, 1H, naphthylic-H) 7.65 (dd, $J = 8.4$ Hz, 1H, naphthylic-H) 7.21 (d, $J = 8.1$ Hz, 1H, naphthylic-H) 4.32 (t, $J = 7.0$ Hz, 2H, ethylene-$C\underline{H}_2$) 3.41 [q, $J = 7.2$ Hz, 4H, $N(C\underline{H}_2CH_3)_2$] 2.66 (t, $J = 7.0$ Hz, 2H, ethylene-$C\underline{H}_2$) 2.37 [s, 6H, $N(C\underline{H}_3)_2$] 1.68 [t, $J = 7.2$ Hz, 6H, $N(CH_2C\underline{H}_3)_2$]. Calculated mass for $[M + H]^+ = 340.44$; observed = 340.1.

Synthesis of A9 (2-[2-(dimethylamino)ethyl]-1H-benz [de]isoquinoline-1,3(2H)-dione)

This compound was synthesized according to the previously published protocols, and similar yields and spectral data were obtained [17]. Calculated mass for $[M + H]^+ = 269.32$; observed = 269.3.

N-acetyl-transferase-2 assay

This assay was performed using a wild-type recombinant human NAT2 (NAT2*4) that was purified from *Escherichia coli* as previously described [22]. The volume of each reaction was 500 µl with 200 µmol/l amonafide, A1 or A2, 100 µg NAT2*4 and 400 µmol/l acetyl CoA (Sigma, Poole, UK). Reactions were run for 0 or 10 min and stopped by the addition of 500 µl of 20% (w/v) trichloroacetic acid (Sigma, Poole, UK) to give a final trichloroacetic acid concentration of 400 µmol/l, which precipitates the enzyme. Two control assays, lacking either enzyme or compound, were performed for each compound. The reaction mixtures were prepared for analysis by isolation of the compounds from the reaction matrix by solid-phase extraction. In brief, 100 µl of the reaction mixture was added to 1 ml of 2% acetic acid. The sorbent of an Oasis HLB 30 mg Extraction Cartridge (Waters Chromatography, Milford, Massachusetts, USA) was conditioned with 1 ml of methanol and 1 ml of water, the prepared sample was applied to the conditioned sorbent, and the sorbent was washed with 1 ml of 5% methanol. Samples were eluted with 200 µl methanol followed by 800 µl of 0.1% formic acid in methanol. The eluant was analyzed by an API 3000 LC-MS/MS system. Samples were infused at 5 µl/min directly into the TurboIonSpray Source (Applied Biosystems), which was operated in the positive ionization mode. The infusions of all samples were subjected to Q1 scans from 150–600 *m/z* AMU with unit resolution. Data are represented as the average ratios of the acetylated compounds to respective the parent compounds from three separate injections. Reactions with no compound were also extracted and injected to ensure that there were no peaks in the reaction mixture that corresponded to the masses of amonafide (284.1 *m/z*), A1 (284.3 *m/z*), A2 (326.6 *m/z*) or the acetylated forms (M + 42.5 *m/z*) thereof (data not shown).

Cell culture

HeLa (cervical carcinoma), WI-38 (normal human skin fibroblasts) and MDA-MB-231 (breast carcinoma), cells

were cultured in Dulbecco's modified Eagle's medium (Invitrogen, Carlsbad, California, USA), and PC-3M (metastatic prostate carcinoma) cells were cultured in RPMI-1640. Peripheral blood mononuclear cells (PBMCs) were voluntarily collected from a healthy laboratory worker by standard sterile phlebotomy techniques and isolated using Vacutainer CPT collection tubes (BD Biosciences, Bedford, Massachusetts, USA). PBMCs were isolated fresh for each experiment. All DMEM and RPMI-1640 media were supplemented with 10% FBS (Atlanta Biologicals, Lawrenceville, Georgia, USA), and 100 U/ml penicillin and streptomycin (Invitrogen). Human umbilical vein endothelial cells (HUVECs) were cultured in endothelial growth medium 2 with supplements provided in the manufacturer's BulletKit (Lonza, Walersville, Maryland, USA). All cells were maintained at 37°C and in a 5% CO_2 atmosphere.

Growth inhibition assays

HeLa, MDA-MB-231, PC-3M, WI-38 and HUVECs were plated at 5000 cells/well in 96-well plates and allowed to attach for 20 h (8 h for HeLa). The media was removed and 198 µl of fresh media was added to each well. Each well was treated with one of 14 doses for each compound (10^5, $10^{4.75}$, $10^{4.5}$, …, $10^{1.75}$ nmol/l) for HeLa cells and with one of eight doses for each compound (10^5, $10^{4.66}$, $10^{4.33}$, …, $10^{2.66}$ nmol/l) for the other cell lines to give a final vehicle concentration of 1% DMSO and a media volume of 200 µl. PBMCs were isolated and plated at 100 000/well in 96-well plates with a volume of 197 µl. They were allowed to settle in the media for 20 h, at which point 1 µl of 1 mg/ml phytohemagglutinin (Sigma, St Louis, Missouri, USA) in phosphate-buffered saline (PBS) was added to stimulate proliferation (final concentration of 5 µg/ml). Each well was treated with one of eight doses for each compound (10^5, $10^{4.66}$, $10^{4.33}$, …, $10^{2.66}$ nmol/l) to give a final vehicle concentration of 1% DMSO and a media volume of 200 µl. Cell proliferation was measured at $t = 0$ (time at start of treatment) and $t = 72$ h using MTS AQueous nonradioactive proliferation assay (Promega, Madison, Wisconsin, USA). This assay uses the metabolic conversion of yellow tetrazolium to a purple formazan by live cells and the color change is proportional to the number of cells [23]. For HeLa, MDA-MB-231, PC-3M, WI-38 and HUVECs, the media was removed and replaced with 120 µl of 1 : 5 v/v MTS: media solution and allowed to incubate for 1 h at 37°C. For PBMCs, 40 µl of the MTS solution was added directly to the media and allowed to incubate for 4 h at 37°C. The absorbance at 490 nm in each well was read with a Spectramax 250 plate reader (Molecular Devices, Sunnyvale, California, USA). The absorbance at $t = 0$ was subtracted from all absorbances at $t = 72$ h so that a 100% growth inhibitory concentration ($[GI_{100\%}]$) corresponds to when $abs_{72\,h} = abs_{0\,h}$. Each experiment was repeated four times, and the data for each concentration were averaged and growth inhibition curves were constructed using XLfit4 software (IDBS, Guildford, UK). Data were fitted to one-site dose–response curves to obtain specific growth inhibitory concentrations and the relative standard errors of the mean for these concentrations were calculated by the XLfit4 software. Statistical significance (P value) for the selectivity and all subsequent assays was determined with the two-tailed homoscedastic Student's t-test. Subsequent assays that use the $[GI_{99\%}]$ are 20 h in duration and assays that use the $[GI_{50\%}]$ are 72 h in duration. GI doses are used in subsequent assays to standardize the effects of the compounds so that the biological responses can be correlated among the different compounds at equitoxic doses.

Subcellular compound localization

HeLa cells were plated at 250 000/35-mm well with a sterile glass coverslip. The cells were allowed to attach for 20 h and were then treated with the $[GI_{99\%}]$ of each derivative for 20 h (total media volume 10 ml/well). The media was removed and the cells were rapidly fixed in 4% w/v paraformaldehyde in PBS for 12 min, permeabilized with 0.5% w/v Triton X-100 in PBS for 5 min, stained with 1.5 mU/µl Texas Red-labeled phalloidin (Invitrogen) for 15 min to mark the cytoplasm (F-actin), counterstained with 50 ng/ml 4′,6-diamidino-2-phenylindole (DAPI) in PBS for 2 min to mark the nuclei (heterochromatin), and then mounted on slides with mounting media (Vector Laboratories, Burlingame, California, USA). The fluorescence of the compounds was detectable in the fluorescein isothiocyanate/green fluorescent protein channel (490–520 nm emission filter) of a Nikon E800 fluorescent microscope (Melville, New York, USA). Images are representative for each compound and were acquired using a 100× objective, SenSys cooled CCD camera (Photometrics, Tucson, Arizona, USA), and MetaView version 4.5 software (Universal Imaging Corp., West Chester, Pennsylvania, USA). Scale bars = 10 µm. DAPI staining was used to bring the nucleus, including the nucleoli, into focus, and this focus plane was used to acquire images in the blue and green channels. The microscope was refocused at the bottom of the cell to acquire images of the phalloidin staining to definitively mark the cytoplasmic boundaries. Images of vehicle-treated cells were acquired with the same exposure, brightness and contrast as compound-treated cells to ensure that the signals in the green channel were not due to the autofluorescence of the cells. The vehicle image in Fig. 3 is representative of these images. A9 does not fluoresce and hence was excluded from this assay.

DNA intercalation assay

A DNA unwinding assay was performed as previously described [1] with minor modifications. Four units of recombinant wild-type human topo I (Topogen, Port Orange, Florida, USA) were incubated with reaction buffer (included with enzyme) and ~0.5 µg of pBR322 plasmid DNA, which is a mixture of form I and form II

plasmid DNA, and water was added to a final volume of 19 µl. The reactions were incubated at 37°C for 30 min, and then 1 µl of each compound was added to give final concentrations of 10, 31.6 and 100 µmol/l (final solvent concentration of 1% DMSO) and the reaction mixture was incubated at 37°C for another 30 min. The reaction was stopped by the addition of 5 µl of gel loading dye [1]. The samples were immediately loaded onto a 1% agarose gel and electrophoresis was performed at 50 V for 3 h at room temperature. Pictures of the gels were obtained using a Kodak Image Station 440 CF (Kodak, Rochester, New York, USA) equipped with a UV source.

In vitro topoisomerase inhibition

HeLa cells were plated at a density of 1.5 million/well in 35-mm wells and allowed to attach for 20 h. They were then treated with each compound at the [$GI_{99\%}$] in 10 ml media for 20 h. In-vitro topo II inhibition was quantified using TopoGEN's Topo II In-vivo Link Kit according to the protocol included with the kit and according to a previously published protocol [24] with slight modifications. In summary, DNA was isolated from sarkosyl-lysed cells, layered onto a cesium chloride gradient (total volume ~7 ml), ultracentrifuged and then fractionated to 0.5 ml. The fractions were diluted 1 : 4 v/v in PBS and the fractions containing the genomic DNA were determined by measuring the absorbance at 260 nm for each fraction. The fractions were then loaded into a slot blotting apparatus and pulled through a nitrocellulose membrane by vacuum. The membrane was blocked in 5% w/v milk in 1 × TBST (blotto) for 2 h, incubated in 1 : 5000 v/v topo II primary antibody (TopoGEN) in blotto for 1 h, washed and incubated in 1 : 2000 v/v horseradish peroxidase (HRP)-conjugated antirabbit secondary antibody (Jackson, West Grove, Pennsylvania, USA) in blotto for 45 min, and washed and developed with SuperSignal West Pico Chemiluminescent Substrate (Pierce, Rockford, Illinois, USA). The data were processed by dividing the intensities of the two or three most intense topo II immunoreactive bands by the amount of DNA in the respective fractions. The band intensity was determined by scanning the developed films with a Kodak Image Station 440 CF, measuring the average pixel intensity of an area slightly larger than each band and subtracting the median background pixel intensity of the perimeter of the same area using Kodak MI software. Etoposide (TopoGEN) and mitoxantrone (Sigma, St Louis, Missouri, USA) are topo II inhibitors used as positive controls. Camptothecin (Sigma, St Louis, Missouri, USA) is a selective topo I inhibitor and was used as negative control. Data were standardized to mitoxantrone in each of three independent experiments.

DNA damage response assay

HeLa cells (250 000) were plated in 35-mm culture dishes and allowed to attach for 8 h, and were then treated with the [$GI_{99\%}$] of each compound for 20 h (total media volume was 10 ml/well with 1% DMSO). After treatment cells were lysed in 150 µl detergent buffer containing 1 : 100 v/v protease inhibitor cocktail (Sigma, St Louis, Missouri, USA). Lysates were run on denaturing 12% acrylamide gels and transferred to nitrocellulose membranes. The membranes were blocked in blotto, incubated in anti-pThr68-Chk2 antibody (Cell Signaling, Danvers, Massachusetts, USA) at 1 : 500 v/v dilution in blotto overnight 4°C, washed, incubated in HRP-conjugated antirabbit secondary antibody (Jackson) at 1 : 5000 v/v dilution in blotto for 1 h and then developed. The membranes were then stripped with a reducing buffer, blocked in blotto, incubated in anti-Chk2 antibody (Biolegend, San Diego, California, USA) at 1 : 500 v/v dilution in blotto overnight at 4°C, washed, incubated in HRP-conjugated antimouse secondary antibody (Jackson) at 1 : 5000 v/v dilution in blotto for 1 h and then developed. Membranes were developed with PicoWest Developing Solution (Pierce) and exposed to film. The intensities of bands were quantified as described in the previous section. The data are expressed as the average ratio of pThr68-Chk2 to total Chk2 as normalized to the mitoxantrone control in each of three independent experiments.

Transwell invasion assay

HeLa cells were plated at 250 000/35-mm well and allowed to attach for 8 h. The cells were washed with PBS and then treated for 4 h with the [$GI_{99\%}$] of each compound (or 1% DMSO, vehicle control) in serum-free media to decrease the number of invading cells in the beginning of the experiment owing to a preliminary lack of drug exposure. The cells were then trypsinized and counted by Trypan blue exclusion with a hemacytometer (Sigma, St Louis, Missouri, USA). Eight-micrometer pore size control well inserts for 12-well plates (BD Biosciences) were coated with 100 µl 1 mg/ml matrigel (Sigma, St Louis, Missouri, USA) and allowed to solidify at room temperature for 1 h. The excess matrigel was aspirated and the inserts were gently washed with PBS. The cells were seeded at a density of 300 000/insert well in a volume of 500 µl serum-free media containing a derivative or vehicle. The inserts were then placed in wells containing 700 µl serum-free media with the respective compound. After 20 h, the cells on the top of the membranes were gently removed with a cotton swab, the membranes then were fixed in methanol for 1 min, stained in Gills No.3 Hematoxylin (Sigma, St Louis, Missouri, USA) for 5 min, rinsed in tap water and allowed to dry overnight. The membranes were excised, mounted on slides and the cells were counted under the 40 × objective of a bright-field microscope. The data are expressed as the average total number of invading cells counted in 20 fields of each membrane, as standardized to the vehicle control, from six experiments.

Perinucleolar compartment reduction

HeLa cells (perinucleolar compartment (PNC) prevalence ~85%) were plated 5000/well in glass-bottomed

96-well plates and allowed to attach for 8 h. The cells were then treated with compounds at the respective [$GI_{50\%}$] for 72 h and [$GI_{99\%}$] for 20 h for each compound (total media volume was 200 µl/well with 1% DMSO). After treatment, cells were immunofluorescently stained as previously described [25], but with a Texas Red-labeled secondary antibody (Jackson) instead of a fluorescein isothiocyanate-labeled secondary antibody. PNC prevalence (% of non-apoptotic/non-mitotic cells with one or more PNCs) was determined by scoring more than 200 cells/well with a fluorescent microscope (60 × objective), and images were acquired with the digital camera and image acquisition software previously mentioned. Scale bar = 10 µm. Data are expressed as the average PNC prevalence (% control) of three individual experiments.

Results and discussion

Chemical synthesis of derivatives

The main rationale for these studies was to produce a derivative of amonafide that could not be metabolized by NAT2 (Fig. 1a) while retaining biological activity in order to potentially dose patients with an amonafide derivative independent of NAT2 genotype or phenotype. We addressed this by creating amonafide derivatives with free or protected amines at the 6-position, instead of the 5-position of amonafide. Amino derivatives at the 6-position were synthesized for several reasons: (i) the chemical synthesis of most derivatives (A2–A8) has not been described, (ii) they are chemically very similar to amonafide compared with previously reported derivatives such as mitonafide, azonafide and elinafide, which do not have arylamines, and (iii) the anticancer properties of these molecules have not been described. The derivatives synthesized were chosen because alkylation of the arylamine would prevent NAT2 acetylation and also to explore the effects of hydrophobicity and primary vs. secondary vs. tertiary arylamines on the biological activity of this class of compounds. A derivative completely lacking the arylamine (A9) was also synthesized as a control to determine the biological significance of the arylamine. The synthesis of A1–A9 was relatively simple and rapid. All reactions were one or two steps from commercial reactants to final product. The hydrogenation of the 6-nitro-imide precursor to produce A1 was the most efficient reaction at 99%, whereas the yield for A2–A9 is between 16 and 91% (Fig. 1b). This ease of synthesis will allow for rapid synthesis of follow-up derivatives in the future if needed.

N-acetyl transferase-2 metabolism of derivatives

To determine whether the novel derivatives were substrates for NAT2, we performed a NAT2 assay that had previously been described [22]. NAT2*4, a rapid acetylating wild-type recombinant protein [22], was used in solution with its coenzyme, acetyl CoA, to determine whether it could acetylate amonafide (positive control), A1 (derivative with a free amine) and A2 (representative negative control with a chemically substituted, or 'blocked,' arylamine). The reaction mixtures were incubated for 10 min, stopped, solid-phase extracted and then injected into a mass spectrometer to determine the extent of *N*-acetylation. Amonafide had undergone extensive acetylation, whereas A2, which lacks the free amine necessary for NAT2 activity, was not acetylated (Fig. 1c). A1 was very minimally acetylated compared with amonafide, demonstrating that simply moving the arylamine to the 6-position successfully blocked the acetylation of this chemotype. This finding could be explained by the arylamine at the 6-postion being less sterically favorable for acetylation in the enzymatic pocket, or by the free amine at the 6-position being less nucleophilic than an amine at the 5-position, or by a combination of both factors. The chemical similarity to amonafide and the inability to be acetylated by NAT2 indicates that these derivatives can be developed as potential replacements for amonafide or as novel anti-cancer drugs that are not metabolized by NAT2.

Growth inhibition and cancer cell selectivity

Derivatives to be considered as potential replacements for amonafide should have similar or better anticancer activities than amonafide. Therefore we first characterized the in-vitro activities of A1–A9 compared with amonafide by constructing growth inhibition curves for three human cancer cell lines (HeLa, PC-3M and MDA-MB-231). The potencies of the derivatives were not greatly affected by the chemical alterations at the 6-position (Fig. 2). A9 still remains fairly potent even though it completely lacks an arylamine, which demonstrates the arylamine is not a necessary molecular feature for growth inhibition in cell lines; however, the derivatives with a primary or secondary amine are the most potent. These data, along with the known metabolic inactivation of amonafide in humans [13] (Fig. 1a) and the previously reported in-vivo potencies of 5-amino derivatives [17], support that the dimethylamino group of the molecule is the most active pharmacophore for growth inhibitory activities. The chemical composition of the amine in the 6-position can, however, affect the selectivity of these compounds. Normal cells (PBMCs, HUVECs and WI-38) were treated with A1–A9 and amonafide to construct GI curves so that the cancer cell selective growth inhibition of the derivatives could be compared with that of amonafide (Fig. 2). PBMCs were chosen as normal cells as the major toxicities associated with amonafide in clinical trials were hematological [4–6,9] and the other cell lines were chosen as they are nontransformed normal primary endothelial and fibroblastic human cells. Amonafide and most of its derivatives are slightly more potent (but not with statistical significance) or equally potent at inhibiting the growth of cancer cells over normal cells. The most hydrophobic derivatives (A5–A7), however, are preferentially inhibiting the growth of normal cells, with A5 doing so significantly ($P < 0.05$),

Fig. 2

(a)

	$[GI_{50\%}] \pm$ SEM (μmol/l)						$[GI_{99\%}]$
	PBMCs	HUVECs	WI-38	HeLa	PC-3M	MDA-MB-231	HeLa
Amn	3.27 ± 0.28	1.35 ± 0.65	5.20 ± 0.79	2.30 ± 0.30	3.31 ± 1.00	2.11 ± 0.49	8.26 ± 2.46
A1	4.63 ± 1.42	4.18 ± 0.92	5.79 ± 0.83	3.25 ± 0.12	5.32 ± 0.85	3.38 ± 0.85	8.88 ± 1.20
A2	3.54 ± 0.43	2.57 ± 0.62	3.94 ± 0.52	2.60 ± 0.19	4.92 ± 0.85	3.46 ± 1.28	8.56 ± 1.53
A3	4.17 ± 0.23	3.31 ± 0.99	4.18 ± 0.37	2.55 ± 0.31	5.50 ± 1.14	3.96 ± 1.05	6.20 ± 1.66
A4	4.11 ± 0.56	1.59 ± 0.42	2.95 ± 0.35	2.42 ± 0.22	3.27 ± 0.27	1.68 ± 0.15	6.86 ± 2.23
A5	1.43 ± 0.12	2.24 ± 0.34	2.31 ± 0.43	3.64 ± 0.22	5.41 ± 0.14	4.06 ± 0.40	6.09 ± 0.85
A6	2.24 ± 0.33	1.38 ± 0.69	2.58 ± 0.45	2.68 ± 0.26	3.63 ± 0.39	2.33 ± 0.36	7.75 ± 1.63
A7	3.69 ± 1.09	2.49 ± 0.48	4.53 ± 0.47	5.90 ± 0.51	6.74 ± 1.17	3.68 ± 0.24	14.33 ± 2.71
A8	11.99 ± 1.51	10.11 ± 1.92	18.75 ± 1.50	9.54 ± 0.63	13.93 ± 1.85	9.63 ± 1.18	21.63 ± 3.14
A9	8.15 ± 1.08	6.65 ± 2.22	10.93 ± 2.21	4.75 ± 0.44	9.56 ± 1.94	5.54 ± 1.03	7.52 ± 1.65

(b)

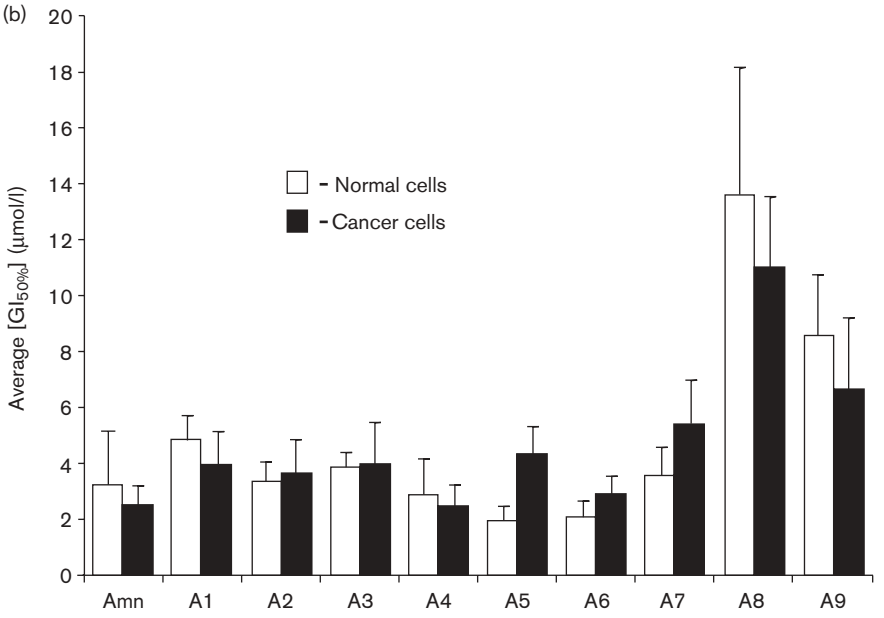

Potencies and selectivity of amonafide (Amn) and derivatives. (a) Growth-inhibition potencies of amonafide and A1–A9 in three human cancer cell lines (HeLa, PC-3M and MDA-MB-231) and three normal human primary cells (PBMCs, HUVECs, and WI-38) as determined by the MTS proliferation assay ($n=4$). Data are reported as the 50% growth inhibitory concentration ± SEM ($[GI_{50\%}] \pm$ SEM) and $[GI_{99\%}] \pm$ SEM for HeLa. (b) Cancer cell selectivity. Data are expressed as the average $[GI_{50\%}]$ for cancer cell lines and average $[GI_{50\%}]$ for normal cells (error bars = + SD).

which suggests that these compounds would not be suitable for further development as anticancer drugs (Fig. 2b). In summary, the in-vitro potencies of 2-[2-(dimethylamino)ethyl]1H-benz[de]isoquinoline-1,3(2H)-diones are not greatly affected by the presence of, or chemical alterations of, a 6-position arylamine; however, the selectivity can be altered by the presence and composition of the amino group in the 6-position.

Subcellular localization of derivatives

Previous studies have shown differential, side chain-dependent, subcellular localization with azonafide derivatives [18,26]; therefore, we determined whether chemical alterations at the arylamine changed the subcellular localization of the 6-amino derivatives, which may affect the biological actions of these compounds. The fluorescence of these compounds can be detected in the green channel (490–520 nm emission filter) of a fluorescent microscope, with the exception of A9, which does not fluoresce. Therefore, we were able to determine the subcellular localization of these compounds in treated and fixed HeLa cells by epifluorescence microscopy. The nucleus and cytoplasm were stained to show the relative distributions of the compounds within the cells (Fig. 3a). All the compounds localize to the nucleus to some extent, but the hydrophobic derivatives (A5–A8) seem to localize

predominantly in the cytoplasmic puncta (Fig. 3). The more hydrophilic compounds (amonafide and A1–A4) localize predominantly to the nucleus, with amonafide, A3 and A4 preferentially localizing to the nucleolus over the nucleoplasm. Subcellular localization patterns do not seem to correlate with the selectivity or potency observed for these compounds. On the basis of the intensity of the fluorescence observed by epifluorescent microscopy and of the yellow hue (color of amonafide and A1–A8 in solution) of cells observed by bright-field microscopy, cells treated with the hydrophobic derivatives (A5–A8) attained much higher cellular concentrations at equi-toxic doses (data not shown). The large cellular build up and poor selectivity of the hydrophobic derivatives (A5–A8) indicate that they might not be as efficacious *in vivo* as they would likely require large doses and hence might cause many side effects before exerting antitumor effects.

Fig. 3

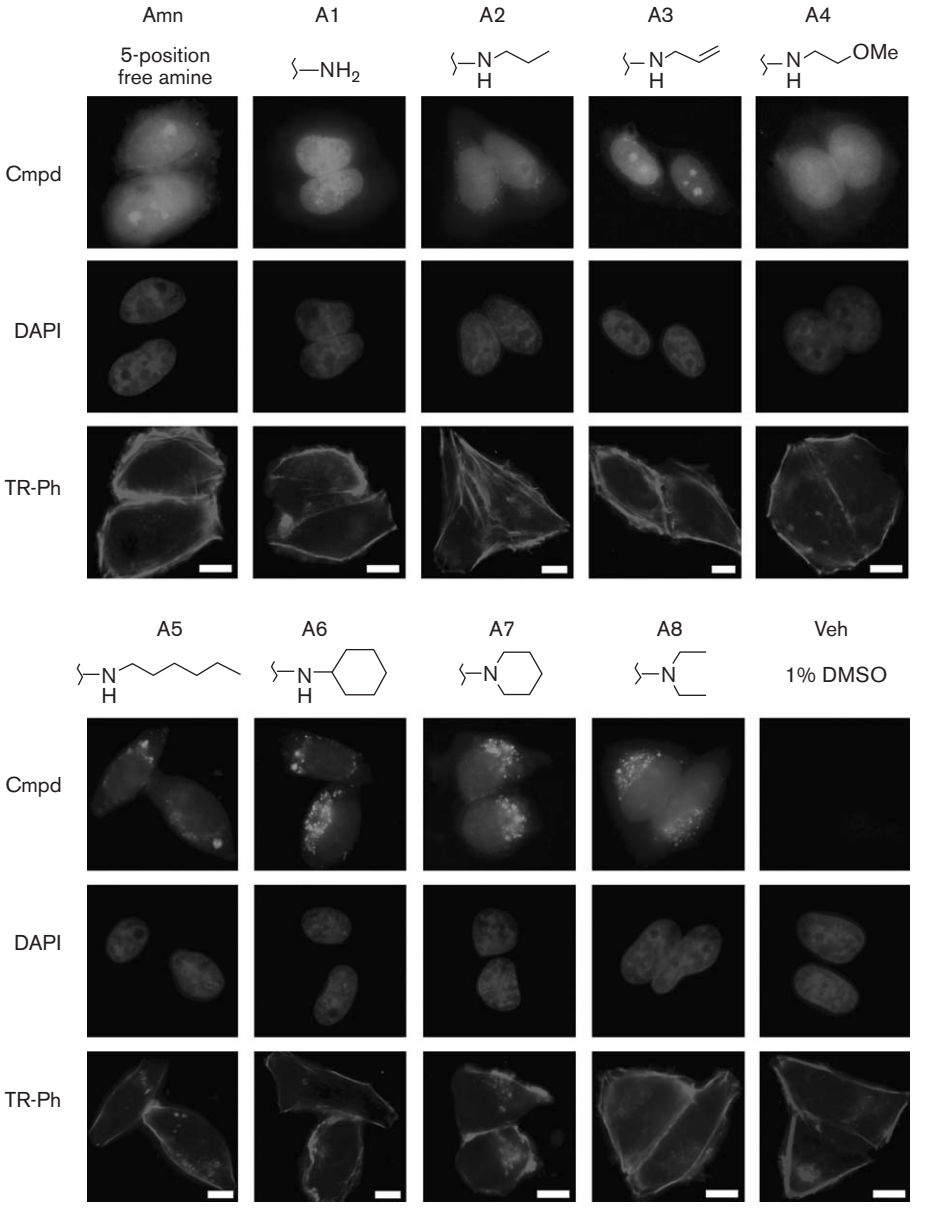

Subcellular localization of amonafide (Amn) and A1–A8. These compounds fluoresce in the green channel; therefore, the signal in the first row represents the relative subcellular localization of each compound (Cmpd). The middle row is the DAPI staining to mark the nucleus and the bottom row is Texas Red–Phalloidin (TR-Ph) staining to mark the boundaries of the cytoplasm. The last column is a representative picture of vehicle-treated cells (Veh) to show that the signals observed in treated cells are not due to autofluorescence of endogenous cellular components. Scale bars = 10 μm. A9 was not included in this figure as it lacks the arylamine and hence does not fluoresce.

DNA intercalation

Amonafide and its structural analogs have been shown to cause topo II-dependent DNA damage in purified systems [1,3]. This activity depends on the ability of these compounds to intercalate DNA, which is the proposed mechanism of cytotoxic action of amonafide and its analogs [1,3]. Therefore, we compared the intercalation of plasmid DNA by A1–A9 with the intercalation by amonafide to determine whether they behave similarly. A topo I-based plasmid DNA unwinding assay was used to determine the intercalation of each compound [1]. If a DNA intercalating agent is added to this reaction, topo I cannot relax the DNA as the DNA writhe will be altered, leading to an equilibrium that favors the form I (supercoiled) DNA. The results of this assay indicate that all the derivatives (A1–A9) do indeed intercalate DNA; however, A5 intercalates much less than the other compounds, followed by the other hydrophobic derivatives (A6–A8) and A1 (Fig. 4). When topo I is absent from the reaction, the DNA band is slightly shifted up on the gel, further supporting the hypothesis that these compounds intercalate DNA.

Topoisomerase II inhibition

Amonafide, mitonafide and azonafide have been all been shown to cause protein-linked DNA breaks *in vitro* [1,18],

Fig. 4

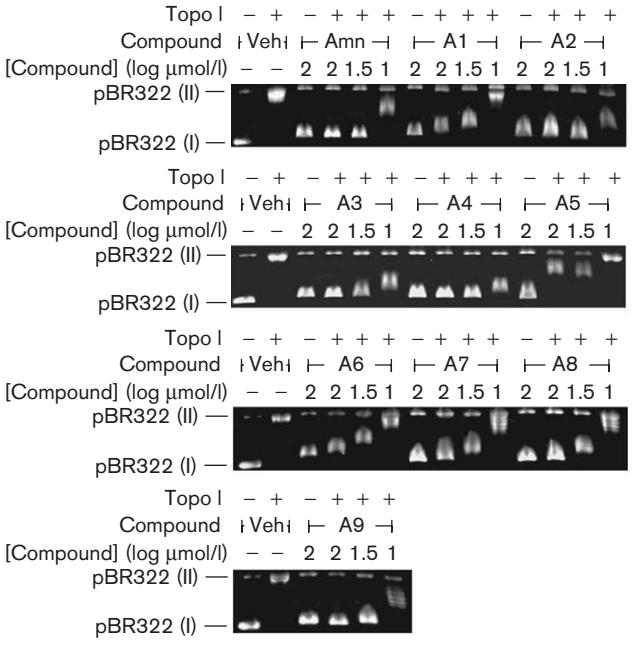

DNA intercalation assay. pBR322 DNA was incubated with three concentrations of each derivative or vehicle (1% dimethyl sulfoxide) and toposiomerase I (topo I; or buffer) was added to each reaction. The topo I enzyme cannot relax DNA with a writhe altered by an intercalating agent. Therefore, compounds that intercalate DNA shift the equilibrium of the reaction towards form I pBR322. Veh, vehicle.

which is considered to be an indicator of topoisomerase inhibition. The mechanism by which these compounds inhibit topo II is, however, not clear. The cytotoxic mechanism of action of most clinically used topo II inhibitors is the stabilization of topo II–DNA cleavable complexes. These complexes can be detected in treated cells after genomic DNA extraction [24] and the detection of such cleavable complexes more directly indicates topo II inhibition than detecting general DNA–protein links. Therefore, we utilized an in-vitro topo II inhibition assay, which detects such topo II–DNA cleavable complexes (Fig. 5a), to determine whether amonafide or A1–A9 inhibit topo II by stabilizing the cleavable complex. In this assay, cells are treated with compounds for 20 h and then lysed to obtain the genomic DNA, and finally the DNA is blotted with topo II antibodies to determine whether any topo II complexes are associated with the DNA. The positive control compounds, mitoxantrone and etoposide, caused the formation of abundant drug-stabilized topo II–DNA cleavable complexes in HeLa cells (Fig. 5a). Camptothecin (a selective topo I inhibitor) was a negative control and did not cause the stabilization of topo II-DNA cleavable complexes (Fig. 5a). The results show that amonafide and A1–A9-treated cells produced very little or no detectable stabilized topo II–DNA cleavable complexes (Fig. 5a). These results suggest that amonafide and structurally related derivatives do not inhibit topo II in cells by the same mechanism as other topo II inhibitors. Our results are consistent with the past finding that amonafide is an ATP-independent inhibitor of topo II, in contrast with other well-characterized and clinically used topo II inhibitors, which are ATP-dependent [27]. These findings suggest that topo II inhibition by amonafide and it derivatives is likely a consequence of the DNA intercalation, but not of the direct inhibition of the topo II enzyme itself. Perhaps the intercalation by this class of compounds stabilizes the DNA breaks caused by topo II, so that they cannot be religated, but does not trap the enzyme on the DNA.

Topoisomerase inhibition by most mechanisms should cause the activation of DNA damage-response pathways because of the production of single and double strand DNA breaks, as is the case with amonafide [3]. It is reasonable to expect that A1–A9 cause the same type of DNA damage as amonafide as dimethylamino-imide is the most active pharmacophore of the amonafide molecule [1] and as this pharmacophore is consistent among the derivatives. Therefore, measuring the DNA damage response at a fixed cytotoxic dose ([$GI_{99\%}$]) will determine the extent to which DNA damage contributes to the cytotoxicity of these compounds. Phosphorylation of Chk2 at threonine68 (Thr68) is an upstream DNA damage response signaling event, subsequent to the activation of ATR/ATM kinases, which are direct responders to DNA damage [28]. Activation of Chk2

was determined by measuring the ratio of pThr68-Chk2 to total Chk2 in HeLa cells treated with the [$GI_{99\%}$]. Amonafide, A2 and A9 evoked the strongest DNA damage response, whereas the most hydrophobic derivatives (A5–A8) caused the least DNA damage response compared with amonafide ($P < 0.1$, Fig. 5b). This data qualitatively correlates with the performance of these compounds in the DNA intercalation assay, which supports the hypothesis that topo II inhibition by these compounds is a result of DNA intercalation rather than the direct inhibition of topo II.

Fig. 5

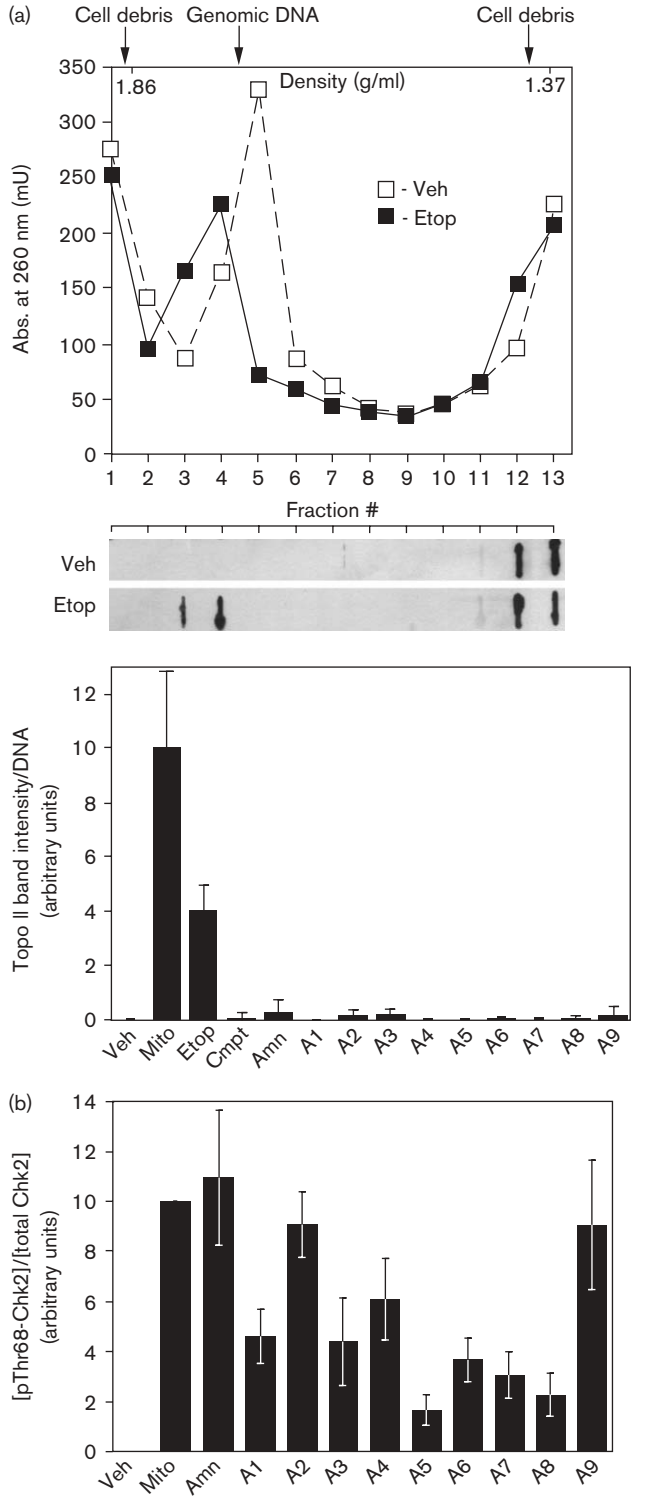

The differential DNA damage response among the derivatives suggests that these compounds might have off-target mechanisms of action or differential downstream affects. The cytoplasmic localization of the hydrophobic derivatives (A5–A8) suggests that these compounds likely have cytotoxic mechanisms of action other than DNA intercalation. We speculate that amonafide derivatives likely bind differential DNA sequences, leading to differential biological impacts. For example, some compounds might preferentially bind gene-rich sequences that are important for cell proliferation and thereby alter the transcription of these genes, leading to a reduction in cellular proliferation, whereas other derivatives might inhibit cell growth mainly through the activation of the DNA damage response pathways, such as Chk2 activation, which inhibit the cell cycle. It is likely that the derivatives inhibit cell growth through differential combinations of these two mechanisms or by other mechanisms.

Effect of derivatives on the malignant phenotype: invasion assay

If A1–A9 have differential targets, DNA-binding specificity, or downstream effects, they might differentially alter the malignant behavior of cells. Moreover, anticancer compounds can be efficacious against tumors in other ways besides inhibiting growth and inducing death of cancer cells; they can also alter the behavior of malignant cells. Therefore, we evaluated the ability of A1–A9 and amonafide to alter the invasive behavior of cancer cells in a transwell (also known as Boyden chamber) invasion assay, which determines the ability of cells to migrate

Fig. 5

In-vitro topoisomerase II (topo II)-inhibition assays. (a) Top panel: example of fractionation and spectrometry to isolate genomic DNA and the correlating slot blot for detection of topo II–DNA crosslinks using a positive (etoposide) and a negative (vehicle, 1% DMSO) control. Bottom panel: quantification of topo II–DNA complexes in HeLa cells treated with 1% DMSO (Veh) or [$GI_{99\%}$] of mitoxantrone (Mito, 1.01 μmol/l), etoposide (Etop, 9.62 μmol/l), camptothecin (Cmpt, 280 nmol/l), amonafide (Amn) and amonafide derivatives (A1–A9). Error bars = + SD ($n = 3$). (b) Quantification of DNA damage response in HeLa cells treated with the [$GI_{99\%}$] by Western blotting for phospho-Thr68 Chk2 and total Chk2 protein. The ratio of activated Chk2 was determined by dividing the intensity of the p-Chk2 bands by the intensity of the Chk2 bands ($n = 3$, error bars = SD). Data from (a) and (b) experiments were normalized to the response of mitoxantrone. DMSO, dimethyl sulfoxide.

through a proteinacious gel. This behavior is considered to be representative of cancer cell invasion through the basement membrane of the primary tumor environment. In this assay, treated cells are seeded on to the top of the matrigel-coated porous membrane, allowed to invade through the proteinacious gel onto the underside of the membrane and then counted. Amonafide, A1, A3 and A8 did not significantly alter the invasive behavior of HeLa cells compared with the control, whereas the other derivatives significantly ($P < 0.05$) decreased the invasiveness of HeLa cells to varying extents (Fig. 6a). The anti-invasive properties of these compounds show no obvious correlations between any of the other data presented here, which demonstrates that these compounds differentially affect cellular behavior and further suggests these derivatives might have differential off-target or downstream effects.

Fig. 6

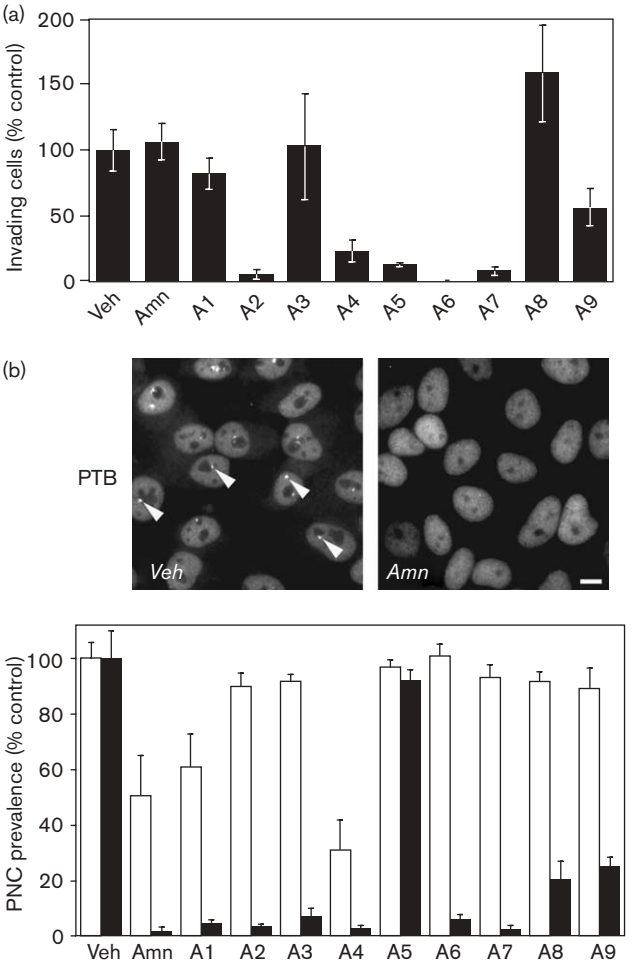

Effect of amonafide and A1–A9 on malignant behavior. (a) Transwell invasion assay quantification. Data were normalized to % invading cells as compared with the vehicle (1% DMSO) control ($n = 6$, error bars = SD). (b) Top panel: HeLa cells treated with 1% DMSO (Veh) or 8.26 μmol/l amonafide (Amn) for 20 h and then immunofluorescently stained with antibodies to PTB (a component of the PNC). PTB localizes to the nucleoplasm (excluding nucleoli) and is highly concentrated in the PNC if present. Exemplary PNCs are marked with arrow heads. Scale bar = 10 μm. Bottom panel: Quantification of PNC prevalence reduction in HeLa cells treated with the [$GI_{50\%}$] (white bar) or the [$GI_{99\%}$] (black bar) of each compound ($n = 3$, error bars = + SD). DMSO, dimethyl sulfoxide; PNC, perinucleolar compartment; PTB, polypyrimidine binding tract protein.

Effect of derivatives on the malignant phenotype: perinucleolar compartment prevalence reduction

We discovered that amonafide was able to eliminate a phenotypic marker of metastatic cells, called the PNC. The PNC is a unique structural marker that it is only found in malignantly transformed cancer cells, irrespective of tissue origin, and indicates cells that are capable of metastasis ([25,29,30] and our unpublished data). This suggests that the PNC is a more comprehensive marker of malignancy than currently used molecular markers of malignancy, which are often cancer type-specific and not directly involved in promoting the malignant behavior. Our previous studies indicate that the PNC likely conveys a functional metastatic advantage to cancer cells ([25,29,30] and our unpublished data). The PNC prevalence (% of cells with one or more PNC) in human breast cancer positively correlates with the progression of the disease and is always near 100% in distant metastases [30]. This suggests that PNC elimination might contribute to the activity of amonafide against advanced/metastatic breast cancers in clinical trials [4–6]. Therefore, we quantified the PNC prevalence reduction of amonafide and A1–A9 for two reasons: (i) to determine the derivatives that would likely be effective against advanced/metastatic cancers, and (ii) to determine whether there was differential PNC-reducing activity among the derivatives and, if so, determine whether it correlated with the other biological activities of these compounds. The PNC prevalence reduction was determined for amonafide and A1–A9 at the respective [$GI_{50\%}$] and [$GI_{99\%}$] doses in HeLa cells, which have a high PNC prevalence of ~85%. At the [$GI_{99\%}$] amonafide and all the derivatives, with the exception of A5, were able to greatly reduce the PNC prevalence (Fig. 6b). Amonafide, A1 and A4 were the only compounds that were able to effectively reduce the PNC at their [$GI_{50\%}$] doses, which suggests that A1 and A4 are the most likely to share that same anticancer properties as amonafide, and potentially have the best efficacy against metastatic cancers. Again, we found that these derivatives caused differential biological responses at fixed cytotoxic doses, which supports differential targets or the downstream effects for these compounds. Moreover, PNC prevalence reduction does not correlate with DNA intercalation, DNA damage response or growth inhibition, which demonstrates that PNC elimination by these derivatives is due to specific molecular interactions of the compounds with cellular targets and not simply a side effect of growth inhibition.

Identification of derivatives for further development

The overall goal of this study was to synthesize and identify a derivative of amonafide that could not be metabolized by NAT2 and which had the potential to be developed as a potential clinical replacement for amonafide or as a novel anticancer agent. Therefore, the derivatives that will be developed further should have biological activities similar to, or better than, amonafide. The data presented here suggest that A4 is the best candidate for further development as it has similar potency and selectivity as amonafide, shows near identical subcellular localization to amonafide, reduces PNC prevalence to the same extent as amonafide at the [$GI_{50\%}$], and greatly decreases invasion compared with amonafide and control. The PNC prevalence reduction and inhibition of invasive behavior by A4 suggests that this compound might be the most efficacious against metastatic and advanced tumors. A1 also deserves further development as its potency, selectivity, subcellular localization, PNC prevalence reduction, chemical structure and physiochemical properties are nearly identical to those of amonafide, which suggests that its biodistribution in animals will be very similar. Although originally included in these studies as a control to determine the biological significance of the 5- and 6-position amines, A9 also deserves further consideration for further development as its potency, selectivity and DNA damage activation are similar to those of amonafide and as it decreases invasive behavior.

Although these 6-amino amonafide derivatives, named here as numonafides, are chemically very similar to amonafide, the small chemical differences between numonafides and amonafide cause differential in-vitro biological activities likely owing to differential off-target, DNA-binding specificities or downstream affects. Moreover, the chemical differences among the derivatives might cause these compounds to become substrates for metabolic enzymes other than NAT2 and CYP1A2, and might differentially affect their biodistribution and clearance in an animal. Therefore, future studies will include in-vivo animal models of human cancer and extensive metabolic studies to test efficacy, toxicity, pharmacodynamics and pharmacokinetics. These studies will determine whether numonafides can potentially replace amonafide in the clinic as a metabolically stable derivative or whether they can be developed as novel anticancer agents.

References

1 Hsiang YH, Jiang JB, Liu LF. Topoisomerase II-mediated DNA cleavage by amonafide and its structural analogs. *Mol Pharmacol* 1989; **36**:371–376.

2 De Isabella P, Zunino F, Capranico G. Base sequence determinants of amonafide stimulation of topoisomerase II DNA cleavage. *Nucleic Acids Res* 1995; **23**:223–229.

3 Andersson BS, Beran M, Bakic M, Silberman LE, Newman RA, Zwelling LA. *In vitro* toxicity and DNA cleaving capacity of benzisoquinolinedione (nafidimide; NSC 308847) in human leukemia. *Cancer Res* 1987; **47**:1040–1044.

4 Scheithauer W, Dittrich C, Kornek G, Haider K, Linkesch W, Gisslinger H, *et al*. Phase II study of amonafide in advanced breast cancer. *Breast Cancer Res Treat* 1991; **20**:63–67.

5 Kornek G, Raderer M, Depisch D, Haider K, Fazeny B, Dittrich C, Scheithauer W. Amonafide as first-line chemotherapy for metastatic breast cancer. *Eur J Cancer* 1994; **30**:398–400.

6 Costanza ME, Berry D, Henderson IC, Ratain MJ, Wu K, Shapiro C, *et al*. Amonafide: an active agent in the treatment of previously untreated advanced breast cancer – a Cancer and Leukemia Group B study (CALGB 8642). *Clin Cancer Res* 1995; **1**:699–704.

7 http://www.xanthus.com/products_xanafide.htm.

8 http://www.chemgenex.com/wt/page/quinamed

9 Ratain MJ, Mick R, Berezin F, Janisch L, Schilsky RL, Williams SF, *et al*. Paradoxical relationship between acetylator phenotype and amonafide toxicity. *Clin Pharmacol Ther* 1991; **50**:573–579.

10 Kreis W, Chan K, Budman DR, Allen SL, Fusco D, Mittelman A, *et al*. Clinical pharmacokinetics of amonafide (NSC 308847) in 62 patients. *Cancer Invest* 1996; **14**:320–327.

11 Innocenti F, Iyer L, Ratain MJ. Pharmacogenetics of anticancer agents: lessons from amonafide and irinotecan. *Drug Metab Dispos* 2001; **29**: 596–600.

12 Taningher M, Malacarne D, Izzotti A, Ugolini D, Parodi S. Drug metabolism polymorphisms as modulators of cancer susceptibility. *Mutat Res* 1999; **436**:227–261.

13 Felder TB, McLean MA, Vestal ML, Lu K, Farquhar D, Legha SS, *et al*. Pharmacokinetics and metabolism of the antitumor drug amonafide (NSC-308847) in humans. *Drug Metab Dispos* 1987; **15**:773–778.

14 Ratain MJ, Rosner G, Allen SL, Costanza M, Van Echo DA, Henderson IC, *et al*. Population pharmacodynamic study of amonafide: a Cancer and Leukemia Group B study. *J Clin Oncol* 1995; **13**:741–747.

15 Ratain MJ, Mick R, Berezin F, Janisch L, Schilsky RL, Vogelzang NJ, *et al*. Phase I study of amonafide dosing based on acetylator phenotype. *Cancer Res* 1993; **53**:2304–2308.

16 Mayr CA, Sami SM, Remers WA, Dorr RT. Identification and characterization of in vitro metabolites of 2-2′-(dimethylamino)ethyl-1,2-dihydro-3H-dibenz-de, h]isoquinoline-1,3-dione. *Drug Metab Dispos* 1998; **26**:105–109.

17 Braña MF, Sanz AM, Castellano JM, Roldan CM, Roldan C. Synthesis and cytostatic activity of benz(de)iso-quinilin-1,3-diones. Structure activity relationships. *Eur J Med Chem – Chim Ther* 1981; **16**:207–212.

18 Mayr CA, Sami SM, Dorr RT. *In vitro* cytotoxicity and DNA damage production in Chinese hamster ovary cells and topoisomerase II inhibition by 2-[2′-(dimethylamino)ethyl]-1, 2-dihydro-3H-dibenz[de,h]isoquinoline-1, 3-diones with substitutions at the 6 and 7 positions (azonafides). *Anticancer Drugs* 1997; **8**:245–256.

19 Braña MF, Castellano JM, Perron D, Maher C, Conlon D, Bousquet PF, *et al*. Chromophore-modified bis-naphthalimides: synthesis and antitumor activity of bis-dibenz[de,h]isoquinoline-1,3-diones. *J Med Chem* 1997; **40**: 449–454.

20 Braña MF, Cacho M, García MA, Pascual-Teresa B, Ramos A, Domínguez MT, *et al*. New analogues of amonafide and elinafide, containing aromatic heterocycles: synthesis, antitumor activity, molecular modeling, and DNA binding properties. *J Med Chem* 2004; **47**:1391–1399.

21 Brana M, Lopez de Arenosa R, Lopez Rodriguez ML, Martinez Sanz Fernandez A. Quantitative structure-toxicity relationships of benzo[d,e]isoquinoline-1,3-diones. *Anal Quim C* 1983; **79**:43–46.

22 Kawamura A, Graham J, Mushtaq A, Tsiftsoglou SA, Vath GM, Hanna PE, *et al*. Eukaryotic arylamine *N*-acetyltransferase. Investigation of substrate specificity by high-throughput screening. *Biochem Pharmacol* 2005; **69**:347–359.

23 Cory AH, Owen TC, Barltrop JA, Cory JG. Use of an aqueous soluble tetrazolium/formazan assay for cell growth assays in culture. *Cancer Commun* 1991; **7**:207–212.

24 Muller MT, Mehta VB. DNase I hypersensitivity is independent of endogenous topoisomerase II activity during chicken erythrocyte differentiation. *Mol Cell Biol* 1988; **8**:3661–3669.

25 Huang S, Deerinck TJ, Ellisman MH, Spector DL. The dynamic organization of the perinucleolar compartment in the cell nucleus. *J Cell Biol* 1997; **137**:965–974.

26 Mayr CA, Sami SM, Remers WA, Dorr RT. Intracellular localization of 6- and 7-substituted 2-[2′-(dimethylamino)ethyl]-1,2-dihydro-3H-dibenz[de,h] isoquino line-1,3-diones (azonafides) is not the limiting factor for their cytotoxicity: an *in vitro* confocal microscopy study. *Anticancer Drugs* 1999; **10**:163–170.

27 Wang H, Mao Y, Zhou N, Hu T, Hsieh TS, Liu LF. Atp-bound topoisomerase ii as a target for antitumor drugs. *J Biol Chem* 2001; **276**:15990–15995.

28 Ahn J, Urist M, Prives C. The Chk2 protein kinase. *DNA Repair (Amst)* 2004; **3**:1039–1047.
29 Kopp K, Huang S. The perinucleolar compartment and transformation. *J Cell Biochem* 2005; **95**:217–225.
30 Kamath RV, Thor AD, Wang C, Edgerton SM, Slusarczyk A, Leary DJ, *et al*. Perinucleolar compartment prevalence has an independent prognostic value for breast cancer. *Cancer Res* 2005; **65**: 246–253.